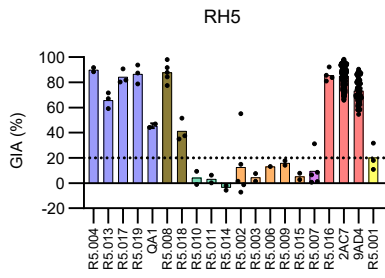
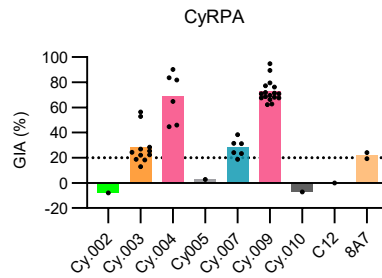
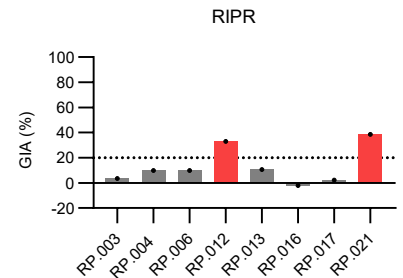
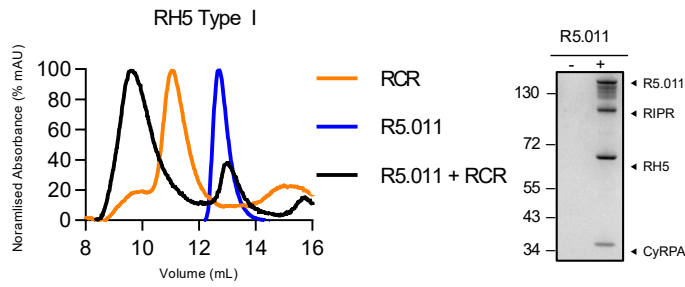
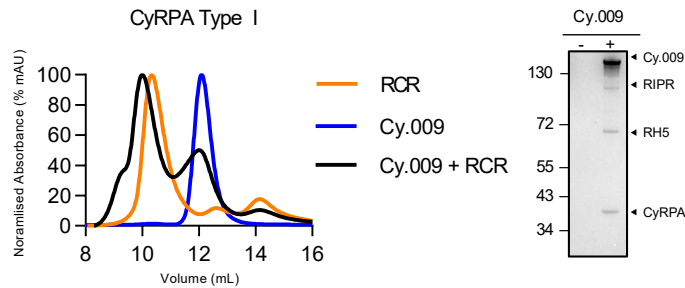
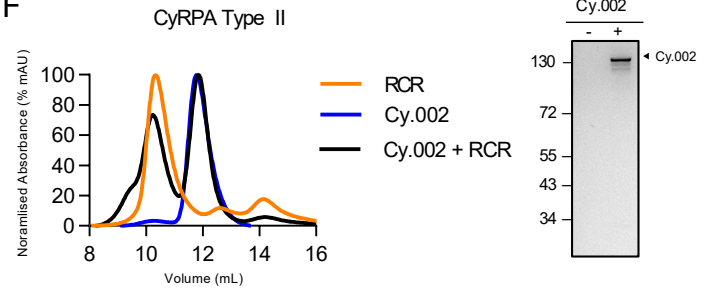
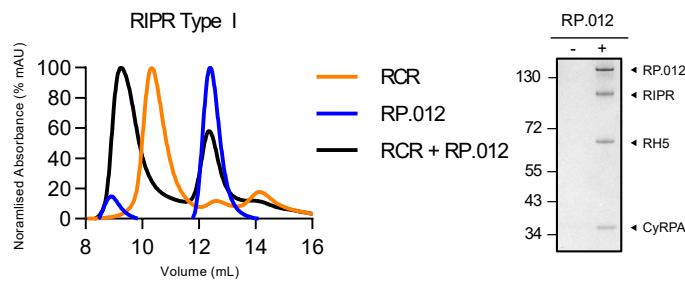
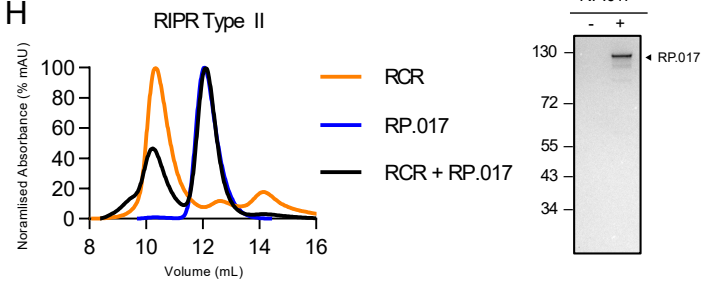


## Development of an improved blood-stage malaria vaccine targeting the essential RH5-CyRPA-RIPR invasion complex – Supplemental information

### Figure S1 – GIA of anti-RH5, -CyRPA, and -RIPR monoclonal antibodies and representative data for mAb interactions with the RCR-complex.

Single cycle GIA assays were performed using *P. falciparum* 3D7 clone parasites. Values reported are analysis at 0.5 mg/mL test mAb concentration unless otherwise stated. **(A)** Anti-RH5 mAbs, colour coded as per epitope bins reported previously<sup>1</sup> and as **Figure 2A**. 2AC7 and 9AD4 were tested at 0.2 mg/mL. **(B)** Anti-CyRPA mAbs colour coded as per epitope bins reported previously<sup>2</sup>. **(C)** Anti-RIPR mAbs colour coded as per **Figure 5A**. Each point is the mean of three technical repeats. Bars show mean values. GIA below the line at 20 % is regarded as negative. **(D)** Size exclusion chromatograms showing complex formation analysis between the RCR-complex and anti-RH5 mAb R5.011 [Type I, GIA-negative] and non-reducing SDS-PAGE gel of co-immunoprecipitation of the pre-formed recombinant RCR-complex without (-) or with (+) mAb R5.011 bound to protein G agarose beads. Other representative examples shown for **(E)** anti-CyRPA mAb Cy.009 [Type I; GIA-positive]; **(F)** anti-CyRPA mAb Cy.002 [Type II; GIA-negative]; **(G)** anti-RIPR mAb RP.012 [Type I; GIA-positive]; and **(H)** anti-RIPR mAb RP.017 [Type II; GIA-negative]. Source data are provided as a Source Data file.

**A****B****C****D****E****F****G****H**

**Figure S2 – Analysis of inter-antigen synergistic GIA of monoclonal antibodies targeting the RCR-complex.**

Full GIA dilution curves of pairwise mAb combinations targeting the RCR-complex. Black: Titrated mAb alone. Red: predicted Bliss additivity GIA for combination of the two mAbs with one held constant at ~30 % GIA. Blue: measured GIA data of the combination of the titrated mAb plus held concentration of the other mAb. Individual points are the mean of a triplicate measurement with error bars indicating the standard deviation. Source data are provided as a Source Data file.





**Figure S3 – Rat immunisation study with full-length RCR-complex antigen combinations.**

Wistar rats were immunised intramuscularly with soluble protein vaccines formulated in Matrix-M™ adjuvant on days 0, 28 and 56. Tail bleeds were taken on day -2 (pre-immunisation) and day 42 (post-second dose), followed by terminal bleed on day 70 (post-third dose). **(A)** Serum IgG ELISA data shown for samples taken on days 42 and 70 against full-length RH5 (red), CyRPA (blue), and RIPR (green) reported in  $\mu\text{g}/\text{mL}$ . Individual and median group responses are shown. Dotted line corresponds to median antigen-specific IgG response from the relevant group of single antigen immunised animals. **(B)** Single-cycle GIA assay using *P. falciparum* clone 3D7. Total IgG was purified from day 70 serum samples and titrated in the GIA assay. Each line represents an individual animal, and each point represents the mean of three technical replicates. GIA at 1 mg/mL total purified IgG was interpolated for each animal. **(C)** Data from (B) replotted against total antigen-specific IgG concentration in  $\mu\text{g}/\text{mL}$  as measured by ELISA in each purified total IgG sample. Each dataset was fitted with a Richard's five-parameter dose-response curve with no constraints to ascertain the  $\text{EC}_{50}$ . Doses of each antigen in  $\mu\text{g}$  used for vaccination are specified in brackets in the title of each graph. Source data are provided as a Source Data file.

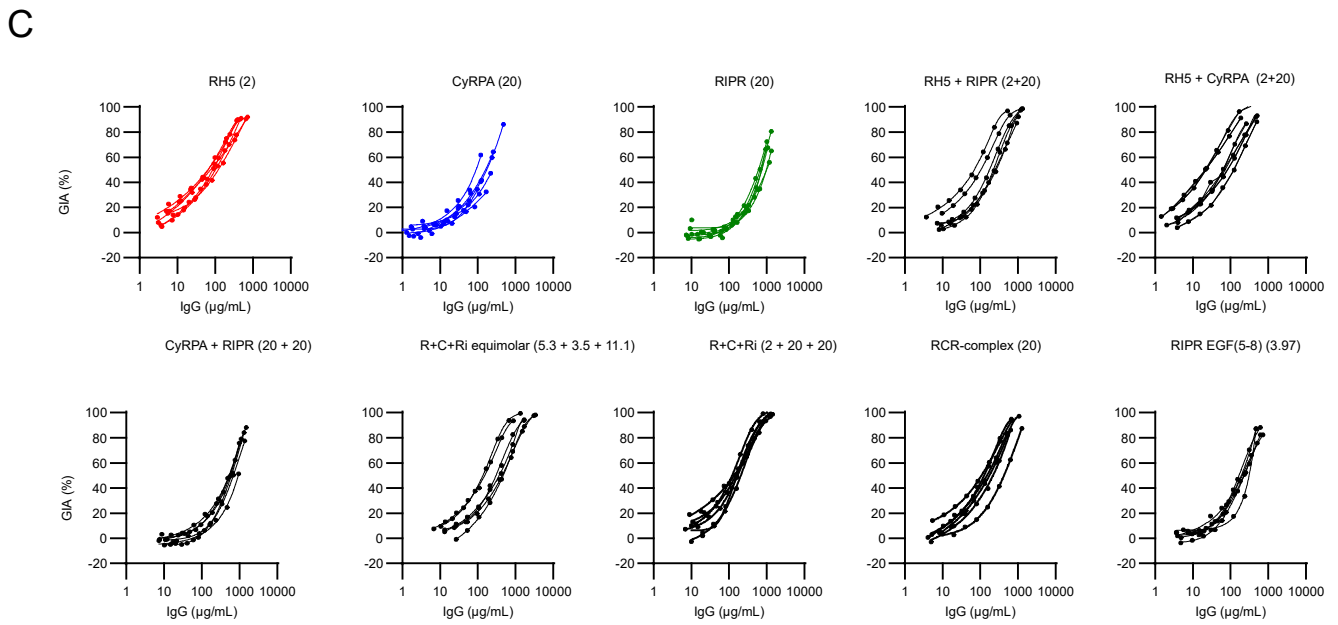
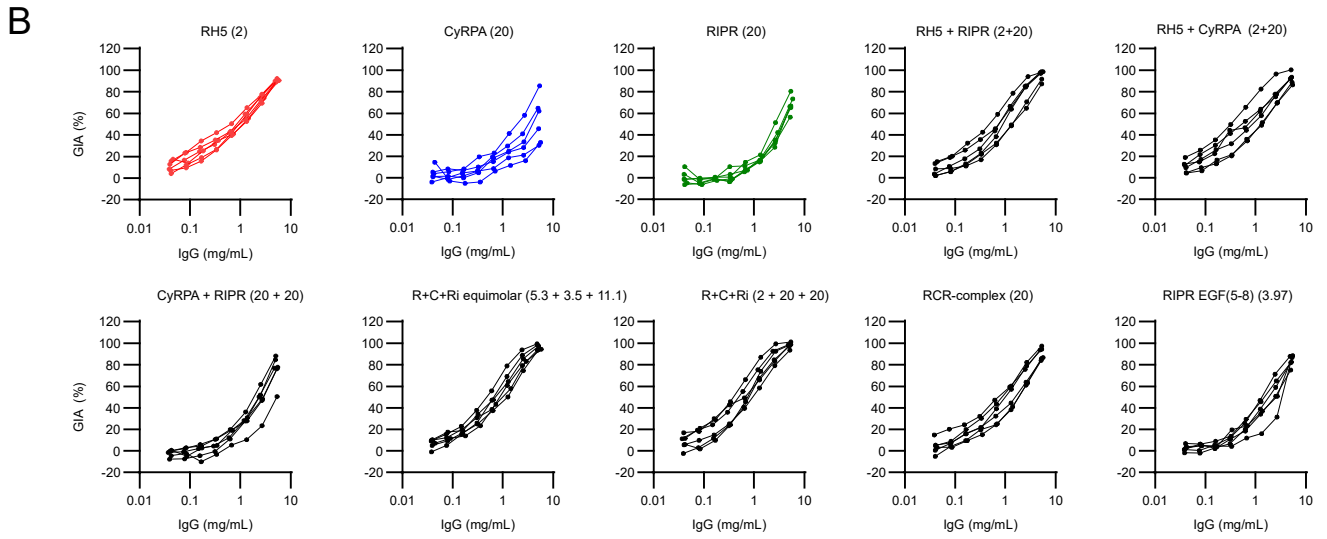
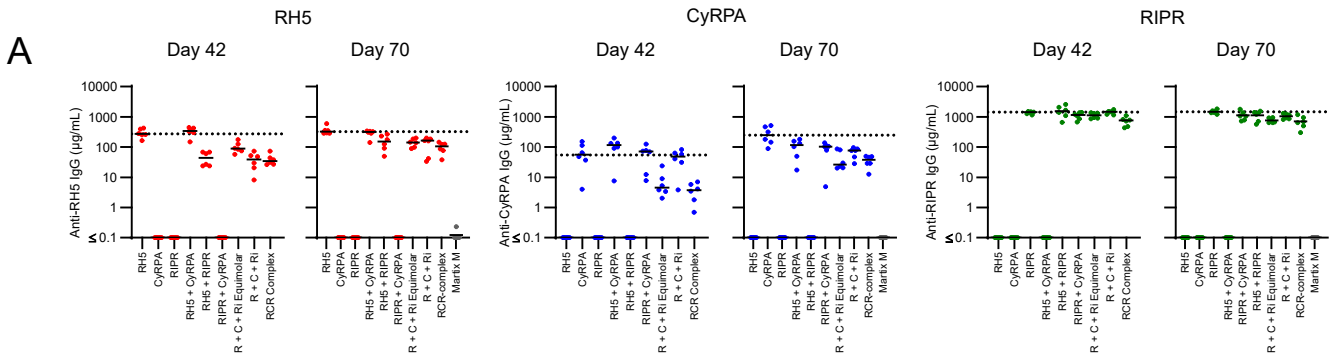
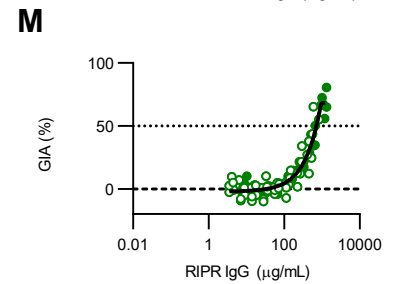
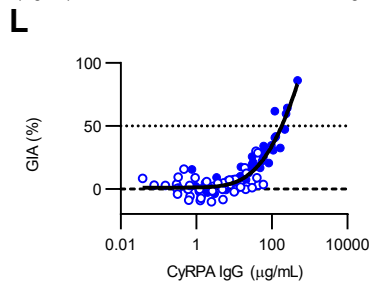
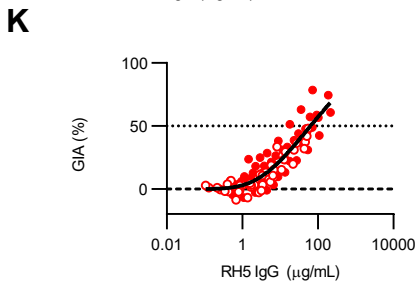
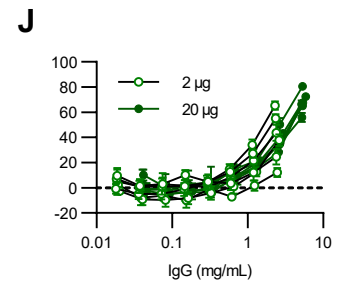
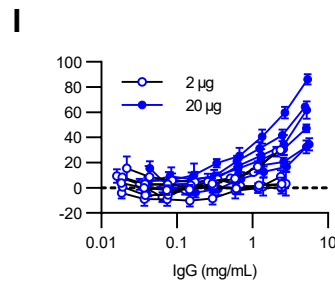
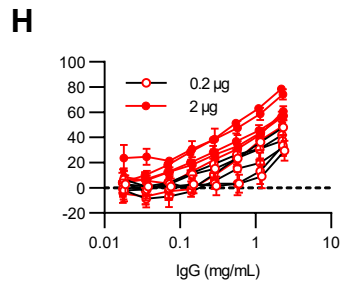
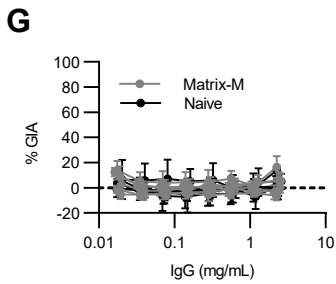
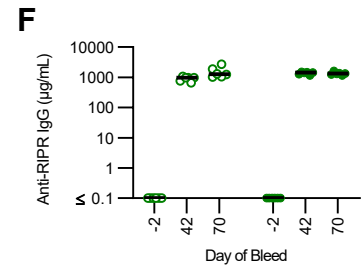
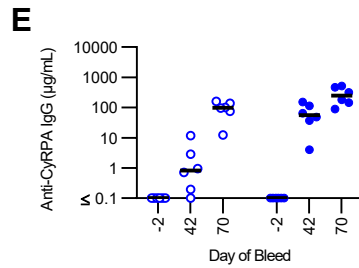
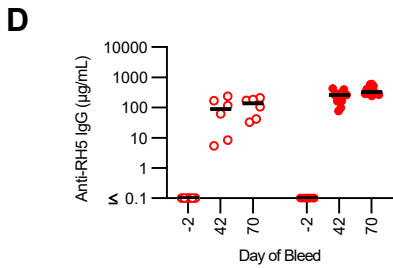
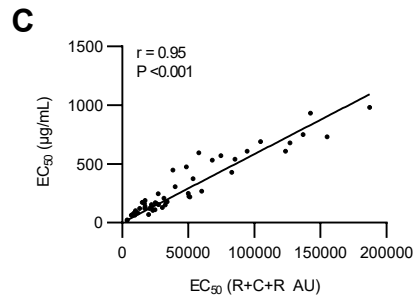
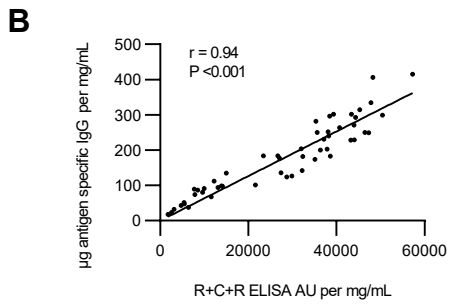
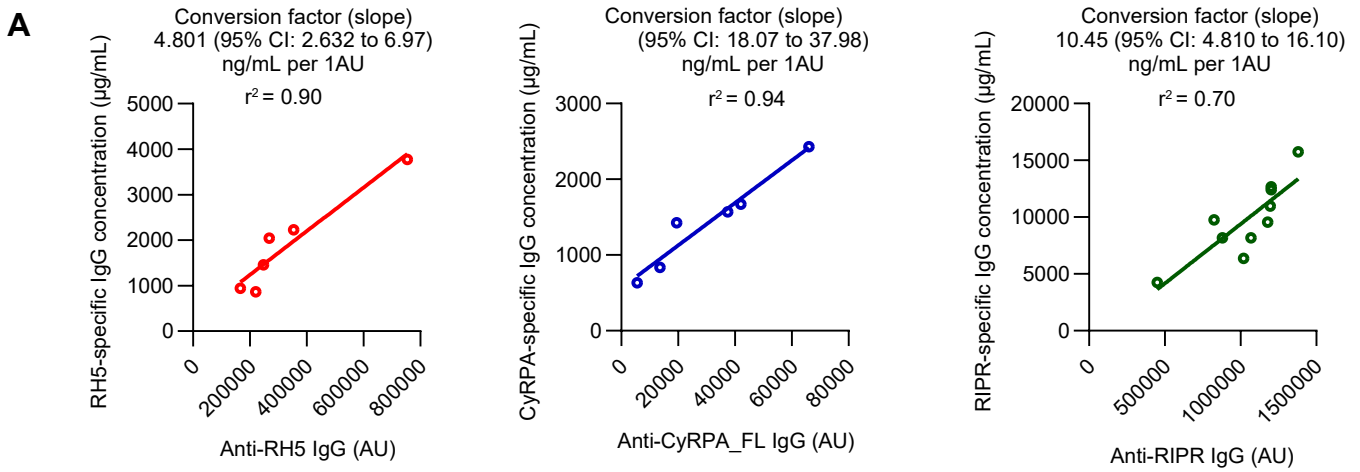


**Figure S4 – Calibration free concentration analysis (CFCA) for rat IgG and rat immunisation study with the single full-length RH5, CyRPA and RIPR antigens.**

(A) CFCA was performed using a Biacore X100 instrument to measure absolute ( $\mu\text{g}/\text{mL}$ ) concentrations of antigen-specific antibody in purified IgG samples from vaccinated rats. Correlation of anti-RH5 IgG (shown in red) measured in arbitrary units (AU) by ELISA for each sample and the RH5-specific IgG concentration measured by CFCA. Linear regression  $r^2$  value is shown (N=6); with the slope used to define the conversion factor between ELISA AU and antigen-specific IgG concentration in  $\text{ng}/\text{mL}$ . The same analysis was repeated for CyRPA (N=6; blue), and RIPR (N=10; green). (B) Correlation of total antigen-specific IgG titers from purified IgG measured using the R+C+R standardised ELISA in arbitrary units (AU) versus the summed total antigen-specific responses in  $\mu\text{g}/\text{mL}$  (derived from independent measurement of responses to the three individual antigens by standardised ELISAs converted to  $\mu\text{g}/\text{mL}$  by CFCA). Significance determined by Pearson's correlation coefficient ( $r$ ). (C) Correlation of interpolated total antigen-specific IgG  $\text{EC}_{50}$  values in the GIA assay derived using the R+C+R ELISA in AU or the summed  $\mu\text{g}/\text{mL}$ . Significance determined by Pearson's correlation coefficient ( $r$ ). (D-F) Serum from Wistar rats immunised three times with full-length antigens formulated in Matrix-M™ adjuvant were tested by ELISA on days -2, 42 and 70 for anti-antigen total IgG responses (reported in  $\mu\text{g}/\text{mL}$ ). (D) Immunisation with 0.2  $\mu\text{g}$  (hollow circles) or 2  $\mu\text{g}$  (filled circles) RH5. (E) Immunisation with 2  $\mu\text{g}$  (hollow circles) or 20  $\mu\text{g}$  (filled circles) CyRPA. (F) Immunisation with 2  $\mu\text{g}$  (hollow circles) or 20  $\mu\text{g}$  (filled circles) RIPR. (G-J) Single cycle GIA assay against *P. falciparum* 3D7 clone using total IgG purified from serum of (G) naïve and Matrix-M™ only immunised rats, (H) RH5, (I) CyRPA, and (J) RIPR immunised animals. (K-M) Functional quality analysis of GIA data from immunisations with full-length RH5, CyRPA or RIPR. Full GIA curves from (H-J) re-plotted against the appropriate anti-antigen specific IgG content of each sample as measured by ELISA in  $\mu\text{g}/\text{mL}$ . N=12 animals per antigen, each dataset fitted with a Richard's five-parameter dose-response curve with no constraints. The dashed line shows 0 % GIA and dotted line shows 50 % GIA for comparison. (N) Summary table of interpolated GIA  $\text{EC}_{50}$  results for each immunisation antigen. Source data are provided as a Source Data file.

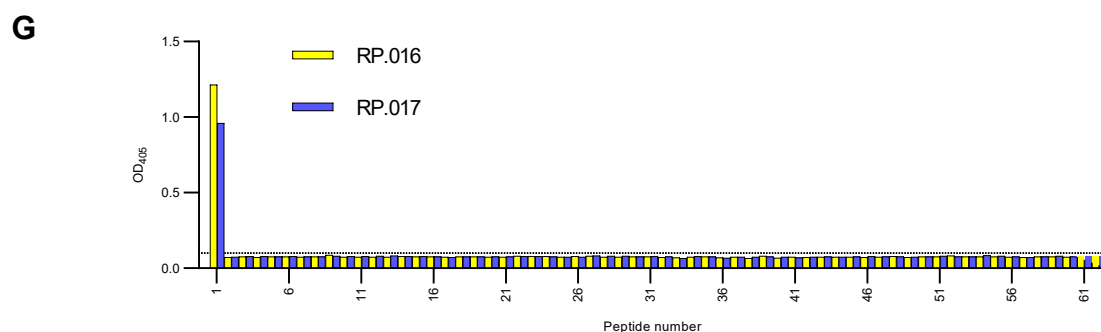
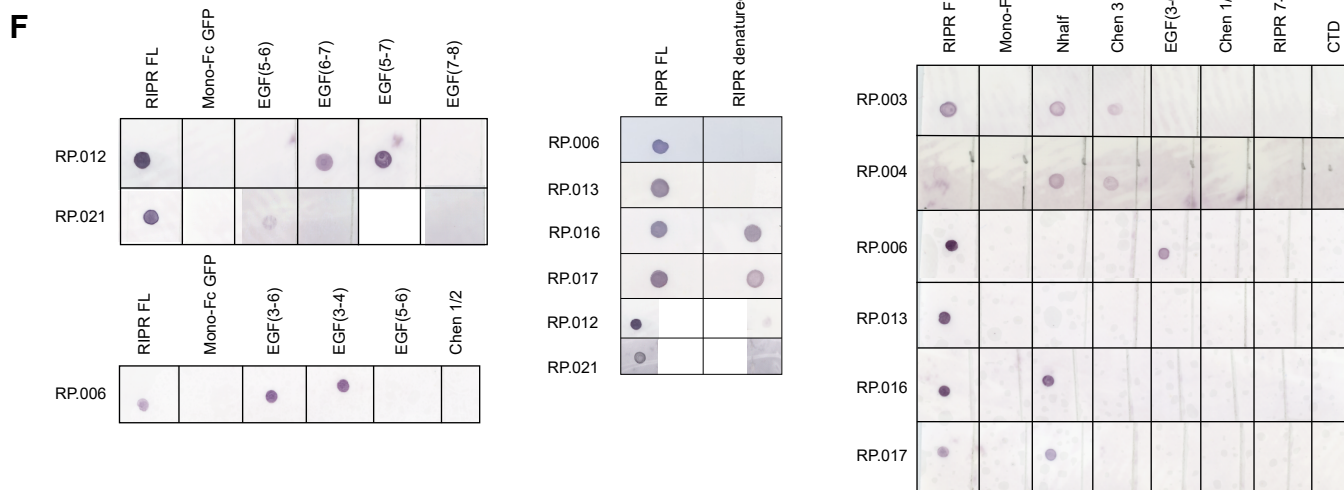
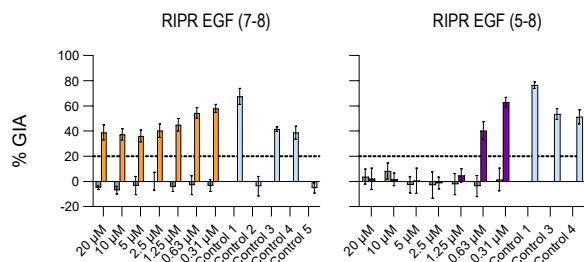
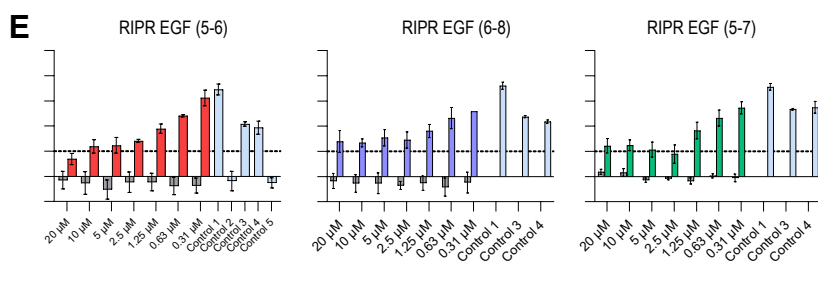
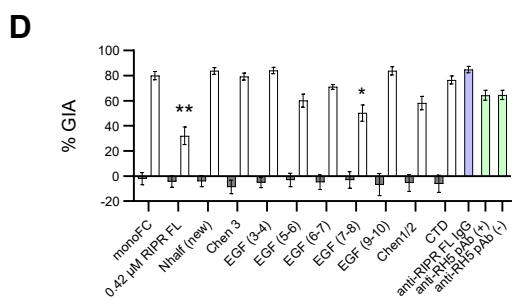
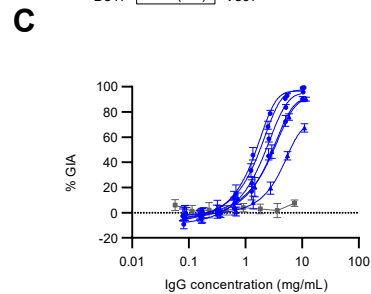
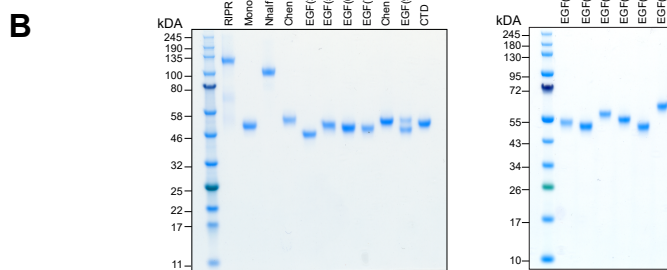
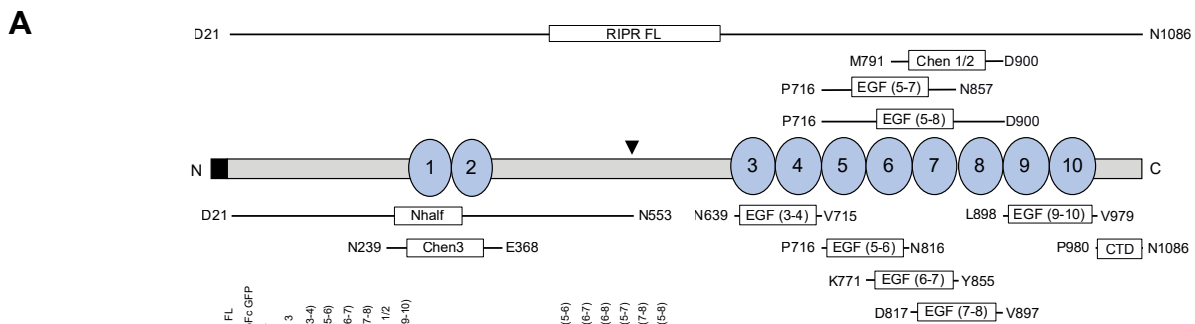


**N**

Antigen	Dose (µg)	EC <sub>50</sub> (µg/mL)	95% CI (µg/mL)
RH5	0.2, 2	64	50 to 89
CyRPA	2, 20	183	165 to 204
RIPR	2, 20	715	669 to 778

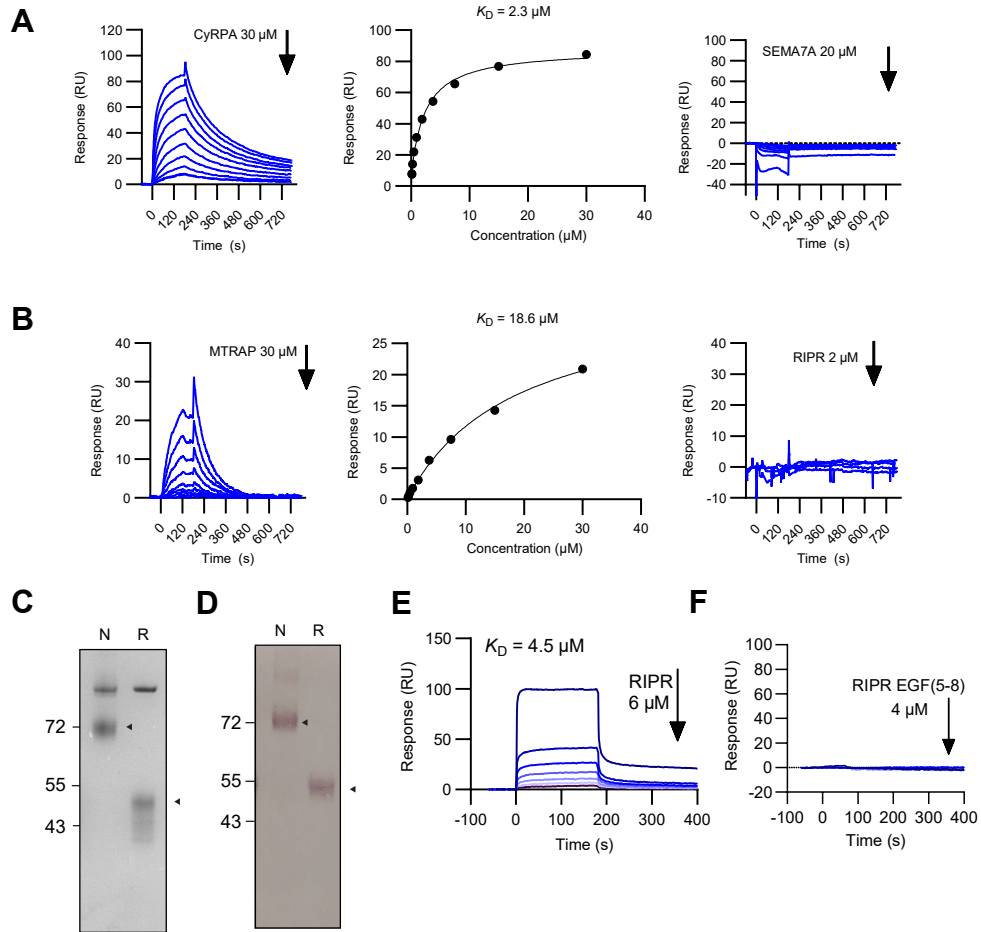
**Figure S5 – Production of RIPR protein fragments, antigen-reversal GIA assays and anti-RIPR mAb epitope mapping.**

(A) Schematic of full-length RIPR protein (RIPR FL) with the design of each RIPR protein fragment labelled with first and last amino acid. EGF domains shown as blue circles. Chen3 and Chen1/2 were previously reported as “Ripr3” and “Ripr1/2” by Chen *et al.*<sup>3</sup> (B) Reducing SDS-PAGE of RIPR FL and RIPR fragments fused to the monoFc prior to cleavage by TEV protease. CTD = C-terminal domain. MonoFc-GFP fusion protein produced as a control. (C) Single cycle GIA assay using *P. falciparum* clone 3D7 of purified IgG from rabbits immunised with full-length RIPR (blue, N=6) or from a pre-immune serum negative control (grey, N=1). Each dataset fitted with a Richard's five-parameter dose-response curve with no constraints. Mean of triplicate wells and SD shown. (D) Antigen reversal single cycle GIA assay using *P. falciparum* clone 3D7 and pooled anti-RIPR IgG from (C). Total purified IgG was held at 3 mg/mL and the indicated RIPR proteins were included at 1  $\mu$ M final concentration unless otherwise indicated. Blue bar = anti-RIPR IgG alone; white bars = anti-RIPR IgG + indicated protein; grey bars = indicated protein alone; green bars = anti-RH5 polyclonal IgG control (pAb) with (+) or without (-) addition of RIPR EGF(7-8) protein. Mean and SD of triplicate wells shown. Significance determined by Kruskal-Wallis test with Dunn's multiple comparison post-test versus anti-RIPR FL IgG alone; \*  $p < 0.05$ , \*\*  $p < 0.01$ . (E) Antigen reversal single cycle GIA assay using *P. falciparum* clone 3D7 and pooled anti-RIPR FL IgG from (C). Total purified IgG was held at 3 mg/mL and the indicated RIPR EGF proteins were titrated from 20  $\mu$ M to 0.31  $\mu$ M final concentration. Coloured bars = anti-RIPR IgG + indicated protein; grey bars = indicated protein alone; blue bars = controls: Control 1 = 3 mg/mL anti-RIPR IgG alone. Control 2 = 20  $\mu$ M RIPR EGF(5-6) or RIPR EGF(7-8) alone. Control 3 = anti-RH5 IgG at 3 mg/mL and Control 4 = 20  $\mu$ M indicated RIPR EGF protein with anti-RH5 IgG at 3 mg/mL. Control 5 = RIPR EGF(5-6) and RIPR EGF(7-8) proteins mixed at 20  $\mu$ M and tested alone. All bars are mean and error bars are SD, N=3 except for EGF(5-8) where N=6. (F) Identification of anti-RIPR mAb binding regions by dot blot using full-length RIPR and indicated RIPR protein fragments. A subset of mAbs were also tested against denatured full-length RIPR protein. (G) Anti-RIPR mAbs RP.016 and RP.017 bound denatured RIPR and Nhalf by dot blot and were then screened on an overlapping peptide ELISA covering amino acids 21-247 and 364-648; both mAbs bind to peptide 1 (IDLIEGIFYEKNEIDKLTFS). Representative graph of two repeats shown. Source data are provided as a Source Data file.



**Figure S6 – Investigation of RIPR interactions with SEMA7A and PTRAMP-CSS.**

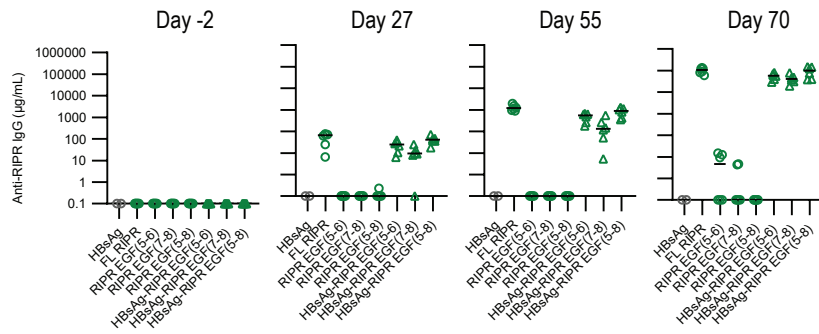
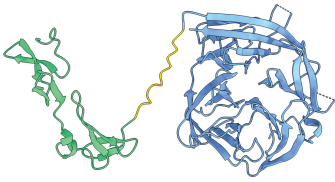
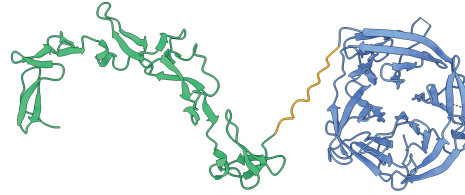
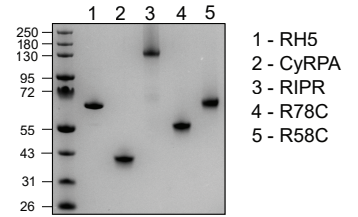
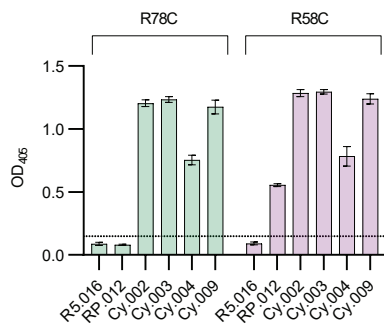
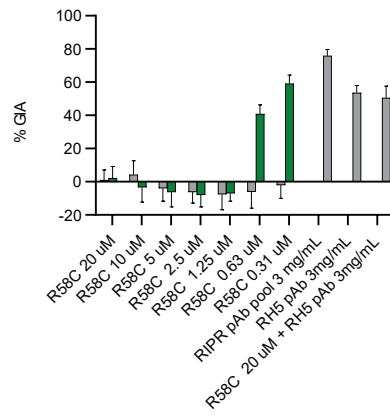
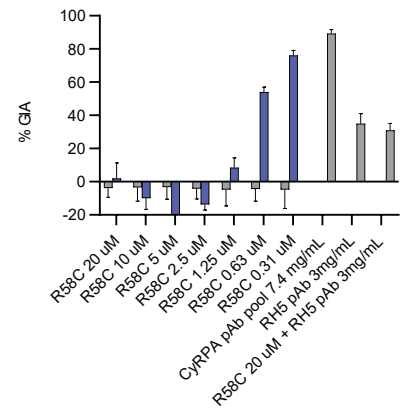
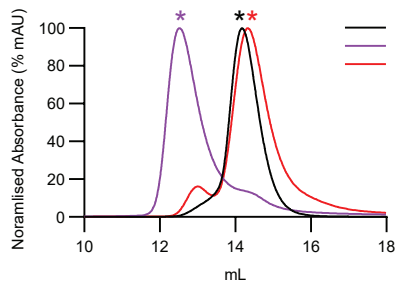
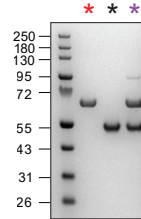
(A) SPR sensorgrams show multi-cycle kinetics of CyRPA (left) or SEMA7A (right) binding to RIPR coated on a CM5 chip. Report points of the equilibrium binding levels of the 9-step 2-fold dilutions for CyRPA binding to RIPR are fitted to the equilibrium or steady-state binding model for  $K_D$  determination (middle). No RIPR binding detected for SEMA7A. (B) SPR sensorgrams show multi-cycle kinetics of MTRAP (left) or RIPR (right) binding to SEMA7A coated on a CM5 chip. Report points of the equilibrium binding levels of the 9-step 2-fold dilutions for MTRAP binding to SEMA7A are fitted to the equilibrium or steady-state binding model for  $K_D$  determination (middle). No SEMA7A binding detected for RIPR. (C) SDS-PAGE gel showing the recombinant PTRAMP-CSS heterodimer run under non-reducing (N) and reducing (R) conditions. Arrows indicate PTRAMP-CSS heterodimer (expected mass 62 kDa, PTRAMP and CSS 31 kDa each), confirmed by mass spectrometry analysis (data not shown). Higher band is an unidentified contaminant from the baculovirus expression system. (D) Western blot of gel shown in (C) using streptavidin-AP to detect biotin added to the BAP tag by BirA. (E) SPR sensorgrams show multi-cycle kinetics of RIPR binding to PTRAMP-CSS heterodimer coated on a CM5 chip. Curves show a 5-step 2-fold dilution series for RIPR binding. The equilibrium or steady-state binding model was used for  $K_D$  determination. (F) No binding of RIPR EGF(5-8) to the PTRAMP-CSS heterodimer could be detected by the same method as (E). Source data are provided as a Source Data file.





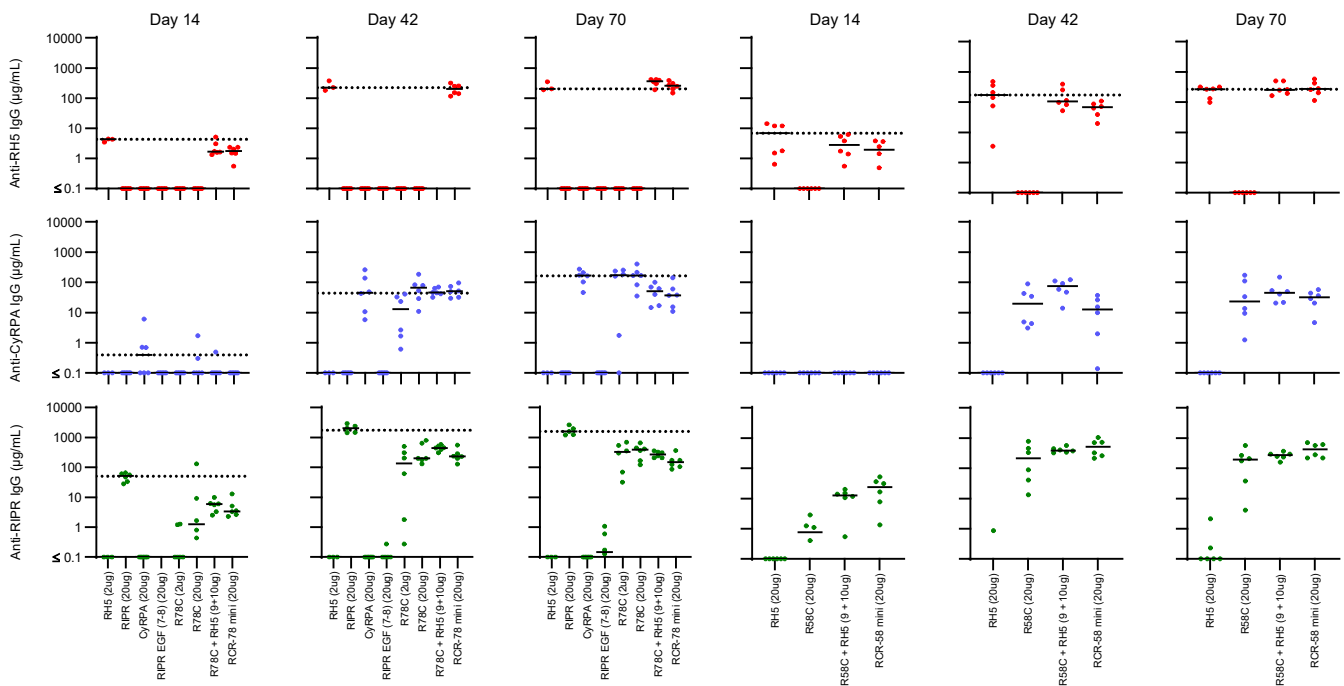
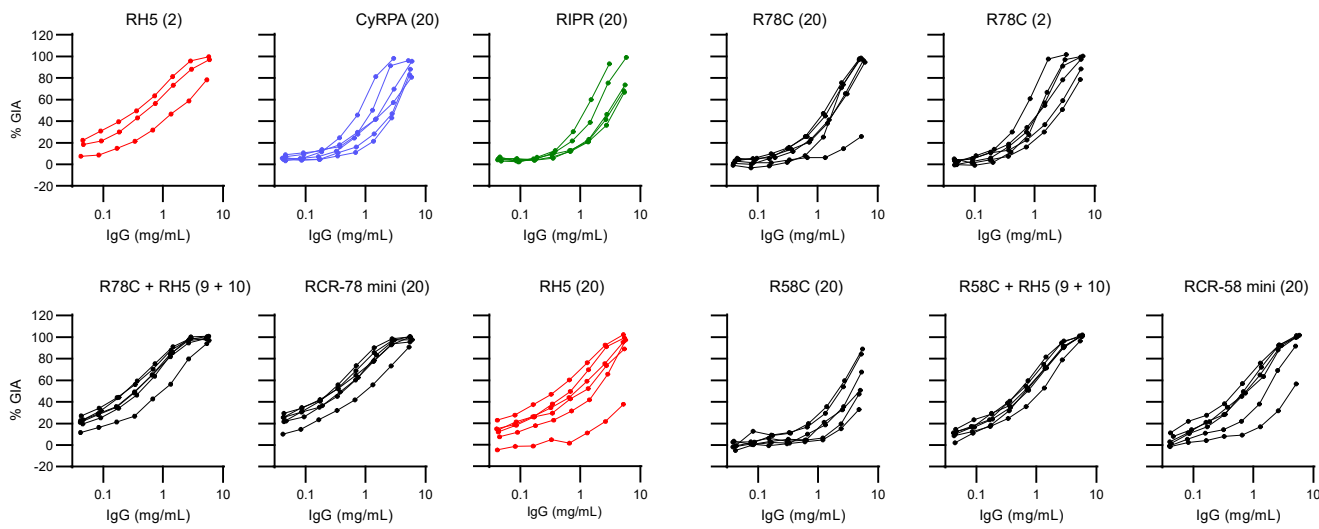
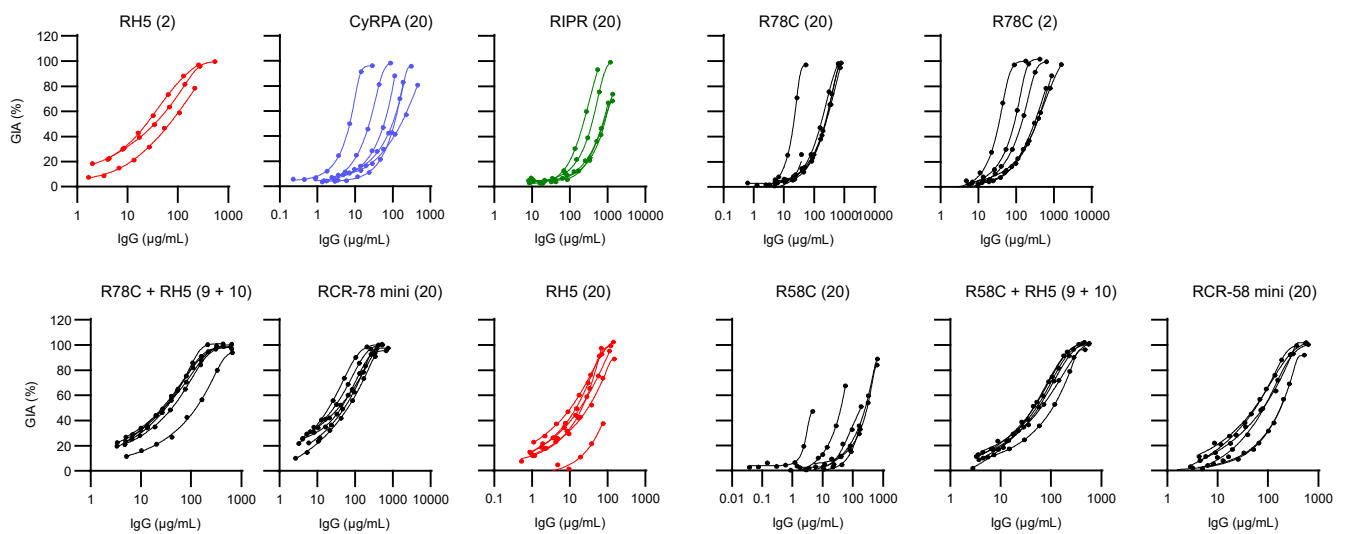
**Figure S7 – Development of vaccines containing RIPR EGF-like domains.**

(A) Wistar rats were immunised three times intramuscularly on days 0, 28 and 56 with full-length (FL) RIPR or the indicated EGF domains as soluble protein vaccines, or with HBsAg VLPs conjugated to the indicated EGF domains or HBsAg VLP control, all formulated in 25 µg Matrix-M™ adjuvant. All doses given as equimolar to 2 µg full-length RIPR. Tail bleeds were taken on day -2 (pre-immunisation), day 27 (post first dose), day 55 (post third dose) and a terminal bleed was taken on day 70. Serum IgG ELISA data shown against full-length RIPR (green) reported in µg/mL. Individual and median group responses are shown. (B) Structural model of R78C. Blue: CyRPA (PDB: 5TIK<sup>4</sup>); orange: linker and SpyTag; green: RIPR EGF(7-8) (AlphaFold<sup>5</sup>). (C) Structural model of R58C. Blue: CyRPA (PDB: 5TIK<sup>4</sup>), orange: linker and SpyTag, green: RIPR EGF(5-8) (AlphaFold<sup>5</sup>). (D) Reducing SDS-PAGE gel of full-length antigens (predicted molecular weights: RH5: 65 kDa, CyRPA: 42 kDa, RIPR 120 kDa), R78C (54 kDa) and R58C (66 kDa). (E) ELISA of a selection of GIA-positive anti-CyRPA, -RIPR, and -RH5 mAbs against R78C and R58C proteins. Error bars are SD (3 technical replicates), dotted line is the negative cut off. (F) Antigen reversal GIA assay using R58C protein and pooled anti-RIPR full-length rabbit IgG from **Figure S5C**, and (G) pooled anti-CyRPA rat IgG from **Figure S4E**. Total purified IgG (polyclonal antibody, pAb) was held at the indicated mg/mL concentration and R58C protein was titrated from 20 µM to 0.31 µM final concentration. Coloured bars = anti-RIPR IgG + R58C protein (green) or anti-CyRPA IgG + R58C protein (blue). Grey bars show indicated protein tested alone, or pAb control, or anti-RH5 pAb IgG negative control with or without 20 µM R58C protein. (H) Size exclusion chromatograms demonstrating complex formation between RH5 and R78C. (I) Non-reducing SDS-PAGE gel assessing binary complex formation between RH5 and R78C. Asterisks on chromatograms indicate which gel lanes correspond to the peaks in (H). Source data are provided as a Source Data file.

**A****B****C****D****E****F****G****H****I**

**Figure S8 – Rat immunisation study with R78C and R58C vaccines.**

Wistar rats were immunised intramuscularly with soluble protein vaccines formulated in 25 µg Matrix-M™ adjuvant on days 0, 28 and 56. Tail bleeds were taken on day -2 (pre-immunisation), day 14 (post-first dose) and day 42 (post-second dose), followed by terminal bleed on day 70 (post-third dose). **(A)** Serum IgG ELISA data shown for samples taken on days 14, 42 and 70 against full-length RH5 (red), CyRPA (blue), and RIPR (green) reported in µg/mL. Individual and median group responses are shown. Dotted line corresponds to median antigen-specific IgG response from the relevant group of single antigen immunised animals where applicable. Data are spread over two graphs to show separate immunisation cohorts. **(B)** Single-cycle GIA assay using *P. falciparum* clone 3D7. Total IgG was purified from day 70 serum samples and titrated in the GIA assay. Each line represents an individual animal, and each point represents the mean of three technical replicates. GIA at 1 mg/mL total purified IgG was interpolated for each animal. **(C)** Data from (B) replotted against total antigen-specific IgG concentration in µg/mL as measured by ELISA in each purified total IgG sample. Each dataset was fitted with a Richard's five-parameter dose-response curve with no constraints to ascertain the EC<sub>50</sub>. Doses in µg of each antigen used for vaccination are specified in brackets in the title on each graph. Source data are provided as a Source Data file.

**A****B****C**

**Table S1 – Details of all monoclonal antibodies used in this study.**NA = Not applicable. NT = Not tested. RH5 epitope bin refers to colour coding reported by Alanine *et al*<sup>1</sup>.

Antigen	mAb name	% GIA at 0.5 mg/mL (3D7)	Type	Epitope bin	mAb Fc species (species origin if applicable)	Isotype used	Reference
RH5	R5.004	89.99	I	Blue	Human	IgG1	Alanine <i>et al.</i> 2019 <sup>1</sup>
	R5.013	65.91	I	Blue	Human	IgG1	Alanine <i>et al.</i> 2019 <sup>1</sup>
	R5.017	84.31	I	Blue	Human	IgG1	Alanine <i>et al.</i> 2019 <sup>1</sup>
	R5.019	86.71	I	Blue	Human	IgG1	Alanine <i>et al.</i> 2019 <sup>1</sup>
	QA1	45.53	I	Blue	Human (Mouse)	IgG1	Douglas <i>et al.</i> 2014 <sup>6</sup>
	R5.008	87.91	I	Brown	Human	IgG1	Alanine <i>et al.</i> 2019 <sup>1</sup>
	R5.018	41.41	I	Brown	Human	IgG1	Alanine <i>et al.</i> 2019 <sup>1</sup>
	R5.010	4.21	I	Green	Human	IgG1	Alanine <i>et al.</i> 2019 <sup>1</sup>
	R5.011	3.37	I	Green	Human	IgG1	Alanine <i>et al.</i> 2019 <sup>1</sup>
	R5.014	0.00	I	Green	Human	IgG1	Alanine <i>et al.</i> 2019 <sup>1</sup>
	R5.002	12.64	II	Orange	Human	IgG1	Alanine <i>et al.</i> 2019 <sup>1</sup>
	R5.003	4.50	II	Orange	Human	IgG1	Alanine <i>et al.</i> 2019 <sup>1</sup>
	R5.006	13.20	II	Orange	Human	IgG1	Alanine <i>et al.</i> 2019 <sup>1</sup>
	R5.009	16.00	II	Orange	Human	IgG1	Alanine <i>et al.</i> 2019 <sup>1</sup>
	R5.015	5.22	II	Orange	Human	IgG1	Alanine <i>et al.</i> 2019 <sup>1</sup>
	R5.007	9.68	II	Purple	Human	IgG1	Alanine <i>et al.</i> 2019 <sup>1</sup>
	R5.016	85.69	I	Red	Human	IgG1	Alanine <i>et al.</i> 2019 <sup>1</sup>
	2AC7	85.54	NT	Red	Human (Mouse)	IgG1	Douglas <i>et al.</i> 2014 <sup>6</sup>
	9AD4	73.53	I	Red	Human (Mouse)	IgG1	Douglas <i>et al.</i> 2014 <sup>6</sup>
	R5.001	20.19	II	Yellow	Human	IgG1	Alanine <i>et al.</i> 2019 <sup>1</sup>
CyRPA	Cy.002	0.00	II	NA	Human (Mouse)	IgG1	Ragotte <i>et al.</i> 2022 <sup>2</sup>
	Cy.003	28.06	I	NA	Human (Chicken)	IgG1	Ragotte <i>et al.</i> 2022 <sup>2</sup>
	Cy.004	68.54	I	NA	Human (Chicken)	IgG1	Ragotte <i>et al.</i> 2022 <sup>2</sup>
	Cy.005	2.68	I	NA	Human (Mouse)	IgG1	Ragotte <i>et al.</i> 2022 <sup>2</sup>
	Cy.007	27.90	I	NA	Human (Chicken)	IgG1	Ragotte <i>et al.</i> 2022 <sup>2</sup>
	Cy.009	74.19	I	NA	Human (Chicken)	IgG1	Ragotte <i>et al.</i> 2022 <sup>2</sup>
	Cy.010	0.00	II	NA	Human (Mouse)	IgG1	Ragotte <i>et al.</i> 2022 <sup>2</sup>
	C12	0.00	NT	NA	Mouse	IgG	Dreyer <i>et al.</i> 2010 & Dreyer <i>et al.</i> 2012 <sup>7,8</sup>
	8A7	21.60	NT	NA	Mouse	IgG1	Chen <i>et al.</i> 2017 <sup>4</sup>
RIPR	RP.003	0.00	II	EGF(1-2)	Mouse	NT	This publication
	RP.004	8.30	II	EGF(1-2)	Mouse	NT	This publication
	RP.006	8.50	I	EGF(3-4)	Mouse	NT	This publication
	RP.012	23.70	I	EGF(6-7)	Mouse	IgG1	This publication
	RP.013	1.40	I	Unknown	Mouse	NT	This publication
	RP.016	0.00	I	Nterm	Mouse	NT	This publication
	RP.017	1.90	II	Nterm	Mouse	NT	This publication
	RP.021	25.80	I	EGF(5)	Mouse	IgG2a	This publication

**Table S2 – Summary statistics for rat immunisation study using full-length RCR antigens.**  
 Summary statistics for ELISA data shown in Figure 4A-C. Sections A-C of the table correspond to Figure 4A-C. Significance determined by one-way ANOVA with Dunnett's multiple comparisons test versus the single antigen only group as indicated, \* p<0.05, \*\*\* p<0.0001, \*\*\*\* p<0.0001, ns = not significant. . One-way ANOVA on log-transformed data with Dunnett's multiple comparison test

<b>Panel A</b>		
<b>Test</b>	<b>Summary</b>	<b>Adjusted P value</b>
RH5 vs. RH5 + CyRPA	ns	0.2311
RH5 vs. RH5 + RIPR	****	<0.0001
RH5 vs. R + C + Ri Equimolar	****	<0.0001
RH5 vs. R + C + Ri	****	<0.0001
RH5 vs. RCR-complex	****	<0.0001
<b>Panel B</b>		
CyRPA vs. RH5 + CyRPA	***	0.0002
CyRPA vs. RIPR + CyRPA	****	<0.0001
CyRPA vs. R + C + Ri Equimolar	****	<0.0001
CyRPA vs. R + C + Ri	****	<0.0001
CyRPA vs. RCR-complex	****	<0.0001
<b>Panel C</b>		
RIPR vs. RIPR + CyRPA	ns	0.0833
RIPR vs. RH5 + RIPR	ns	0.0819
RIPR vs. R + C + Ri Equimolar	****	<0.0001
RIPR vs. R + C + Ri	*	0.0187
RIPR vs. RCR-complex	****	<0.0001

**Table S3 – Summary statistics for rat immunisation study using R58C and R78C antigens.**

Summary statistics for ELISA data shown in Figure 6A-F. Sections A-F of the table correspond to Figure 6A-F. Significance determined by one-way ANOVA of data with Dunnett's multiple comparisons test versus the single antigen only group as indicated, \* p<0.05, \*\* p<0.001, \*\*\*\* p<0.0001, ns = not significant.

Panel A		
Test	Summary	Adjusted P Value
RH5 (2ug) vs. CyRPA (20ug)	****	<0.0001
RH5 (2ug) vs. RIPR (20ug)	****	<0.0001
RH5 (2ug) vs. RIPR EGF (7-8)(20ug)	****	<0.0001
RH5 (2ug) vs. R78C (2ug)	****	<0.0001
RH5 (2ug) vs. R78C (20ug)	****	<0.0001
RH5 (2ug) vs. R78C + RH5 (9+10ug)	ns	0.0534
RH5 (2ug) vs. RCR-78 mini (20ug)	ns	0.9971
Panel B		
Test	Summary	Adjusted P Value
RH5 (20ug) vs. R58C (20ug)	****	<0.0001
RH5 (20ug) vs. R58C + RH5 (9+10ug)	ns	0.5648
RH5 (20ug) vs. RCR-58 mini (20ug)	ns	0.6526
Panel C		
Test	Summary	Adjusted P Value
CyRPA (20ug) vs. RH5 (2ug)	****	<0.0001
CyRPA (20ug) vs. RIPR (20ug)	****	<0.0001
CyRPA (20ug) vs. RIPR EGF (7-8)(20ug)	****	<0.0001
CyRPA (20ug) vs. R78C (2ug)	ns	0.1818
CyRPA (20ug) vs. R78C (20ug)	ns	>0.9999
CyRPA (20ug) vs. R78C + RH5 (9+10ug)	ns	0.4637
CyRPA (20ug) vs. RCR-78 mini (20ug)	ns	0.3631
Panel D		
Test	Summary	Adjusted P Value
CyRPA vs. RH5 (20ug) <sup>†</sup>	****	<0.0001
CyRPA vs. R58C (20ug) <sup>†</sup>	*	0.0113
CyRPA vs. R58C + RH5 (9+10ug) <sup>†</sup>	ns	0.1636
CyRPA vs. RCR-58 mini (20ug) <sup>†</sup>	*	0.0208
Panel E		
Test	Summary	Adjusted P Value
RIPR (20ug) vs. RH5 (2ug)	****	<0.0001
RIPR (20ug) vs. CyRPA (20ug)	****	<0.0001
RIPR (20ug) vs. RIPR EGF (7-8) (20ug)	****	<0.0001
RIPR (20ug) vs. R78C (2ug)	**	0.0012
RIPR (20ug) vs. R78C (20ug)	*	0.0103
RIPR (20ug) vs. R78C + RH5 (9+10ug)	**	0.0045
RIPR (20ug) vs. RCR-78 mini (20ug)	***	0.0002
Panel F		
Test	Summary	Adjusted P Value
RIPR vs. RH5 (20ug) <sup>‡</sup>	****	<0.0001
RIPR vs. R58C (20ug) <sup>‡</sup>	***	0.0005
RIPR vs. R58C + RH5 (9+10ug) <sup>‡</sup>	*	0.0224
RIPR vs. RCR-58 mini (20ug) <sup>‡</sup>	ns	0.088

<sup>†</sup>Performed on CyRPA data from panel C

<sup>‡</sup> Performed on RIPR data from panel E

Table S4 – Details of PCR primers used to make RIPR truncations.

Name	Sequence	Target	Amino Acid coordinate	Enzyme sites	Orientation
NhalfCoFW	gatcggatccGATCTGATCGAGGGCATCTT	Codon optimised (3133) Nhalf (NH)	21	4 Bases-BamHI-Ripr	FW
NhalfCoRV	gatcgggtaccaccGTTAGAGTTGGTGTGGGGGT	Codon optimised (3133) Nhalf (NH)	533	4 Bases-KpnI-G-Ripr	RV
BGWP007	gatcggatccAATATCAACAACATGAATAT	CO PfRipr (5285) Chalf region (CH)	534	4 Bases-BamHI-Ripr	FW
BGWP008	gatcgggtaccaccGTTCTGGTTGGAGTAATAGA	CO PfRipr (5285) Chalf region (CH)	1086	4 Bases-KpnI-G-Ripr	RV
BGWP009	gatcggatccCGGTGCACCCAGGACATCTG	CO PfRipr (5285) EGF1-2 (E12D)	287	4 Bases-BamHI-Ripr	FW
BGWP010	gatcgggtaccaccGTAGCACTTGTGTTGTGGT	CO PfRipr (5285) EGF1-2 (E12D)	362	4 Bases-KpnI-G-Ripr	RV
BGWP013	gatcggatccAACCTGTGCAACAAGTGCA	CO PfRipr (5285) EGF3-10 (E310D)	639	4 Bases-BamHI-Ripr	FW
BGWP014	gatcgggtaccaccCACGCAGCTGTCGTCCTGT	CO PfRipr (5285) EGF3-10 (E310D)	979	4 Bases-KpnI-G-Ripr	RV
BGWP015	gatcggatccCCCAACACCAACGAGTACGACGA	CO PfRipr (5285) CTD	980	4 Bases-BamHI-Ripr	FW
BGWP019	gatcggatccAACATCCAGTACCAGTGCAT	CO PfRipr (5285) Chen3	238	4 Bases-BamHI-Ripr	FW
BGWP020	gatcggatccAACGAAGAGACAGACATCGT	CO PfRipr (5285) Chen1/2	791	4 Bases-BamHI-Ripr	FW
BGWP021	gatcgggtaccaccATCTTCCAGCACGCACTTCC	CO PfRipr (5285) Chen1/2	900	4 Bases-KpnI-G-Ripr	RV
BGWP022	gatcgggtaccaccATTGAGGATGCACTCGCCTC	CO PfRipr (5285) EGF3-6 (E36D)	816	4 Bases-KpnI-G-Ripr	RV
BGWP023	gatcggatccGACTACTGCAAGGACATCAA	CO PfRipr (5285) EGF 7-10 (E710D)	817	4 Bases-BamHI-Ripr	FW
BGWP042	gatcgggtaccaccCACGCATTTGCCCTTTCACGT	CO PfRipr (5285) E34D	716	4 Bases-KpnI-G-Ripr	RV
BGWP043	gatcggatccCCCGATAACAAGTGCACCT	CO PfRipr (5285) E56D	716	4 Bases-BamHI-Ripr	FW
BGWP044	gatcgggtaccaccCACGCACTTCCCCTTTCACGG	CO PfRipr (5285) E78D	897	4 Bases-KpnI-G-Ripr	RV
BGWP045	gatcggatccCTGGAAGATAAGTGCCTGCA	CO PfRipr (5285) E910D	898	4 Bases-BamHI-Ripr	FW
BGWP054	gatcgggtaccaccGTTTTTGGCAATGCAGTTGA	CO PfRipr (5285) EGF 5	770	4 Bases-KpnI-G-Ripr	RV
BGWP055	gatcggatccAAGTGAAGCGGAAAGAGTA	CO PfRipr (5285) EGF 6	771	4 Bases-BamHI-Ripr	FW
BGWP056	gatcgggtaccaccATAGATGCACTCCCCCTTGT	CO PfRipr (5285) EGF 7	855	4 Bases-KpnI-G-Ripr	RV
BGWP057	gatcggatccGAGAACAGCTGCCTGATCAA	CO PfRipr (5285) EGF 8	856	4 Bases-BamHI-Ripr	FW
BGWP068	gatcggatccGCCAAAACAAGTGCAGCG	CO PfRipr (5285) EGF 6	768	4 Bases-BamHI-Ripr	FW
BGWP069	gatcgggtaccaccGTCATTGAGGATGCACTCGC	CO PfRipr (5285) EGF 6	817	4 Bases-KpnI-G-Ripr	RV
BGWP070	gatcggatccCTGAATGACTACTGCAAGGA	CO PfRipr (5285) EGF 7	815	4 Bases-BamHI-Ripr	FW
BGWP071v2	gatcgggtaccaccGTTCTCATAGATGCACTCCC	CO PfRipr (5285) EGF 7	857	4 Bases-KpnI-G-Ripr	RV
BGWP072	gatcggatccTATGAGAACAGCTGCCTGAT	CO PfRipr (5285) EGF 8	855	4 Bases-BamHI-Ripr	FW
BGWP073	gatcgggtaccaccATCTTCCAGCACGCACTTCC	CO PfRipr (5285) EGF 8	900	4 Bases-KpnI-G-Ripr	RV
BGWP074	gatcggatccCTGGAAGATAAGTGCCTGCA	CO PfRipr (5285) EGF 9	989	4 Bases-BamHI-Ripr	FW
BGWP075	gatcgggtaccaccATTCTGGATCAGGCACACGC	CO PfRipr (5285) EGF 9	941	4 Bases-KpnI-G-Ripr	RV
BGWP076	gatcgggtaccaccGGTGAAGCTCTGCTGTACT	CO PfRipr (5285) EGF 10	990	4 Bases-KpnI-G-Ripr	RV



**Table S5 – Details of RIPR truncations produced.**

RIPR fragment description	Amino acids	Expression in Expi293 cells	MS/MS verified	Intact mass verified
monoFc + GFP	N/A	✓	✓	✓
monoFc + N-half	D21-N553	✓	✓	✗
monoFc + Chen3	N239-E368	✓	✓	✓
monoFc + EGF domains 3-6	N639-N816	✓	✓	✓
monoFc + Chen1/2	N791-D900	✓	✓	✓
monoFc + EGF domains 7-10	D817-V979	✓	✓	✓
monoFc + EGF domains 3-4	N639-V715	✓	✓	✓
monoFc + EGF domains 5-6	V716-N816	✓	✓	✓
monoFc + EGF domains 6-7	K771-Y855	✓	✓	✓
monoFc + EGF domains 7-8	D817-V897	✓	✓	✓
monoFc + EGF domains 9-10	L898-V979	✓	✓	✓
monoFc + EGF domains 5-8	V716-D900	✓	✓	✓
monoFc + EGF domains 5-7	V716-N857	✓	✓	✓
monoFc + EGF domains 3-6	K771 - N816	Poor	✓	✗
monoFc + EGF domains 7-10	D817 - V979	Poor	✓	✗
monoFc + C-terminal domain	P980-N1086	✓	✓	✓

**Table S6 – Amino acid sequences of R78C and R58C**

Protein	Amino acid sequence (signal peptide underlined).
R78C	<u>MGWSCIIIFLVATATGVHSDYCKDINCKENEECSIVNFKPECVCKENLKKNNKGECIYENSCL</u> INEGNCPKDSKCIYREYKPHECVCKENKQGHVAVNGKCVGGGGSGGGGSAHIVMVDAYKPTK GGGGSGGGGSDSRHVFIRTELSFIKNNVPCIRDMFFIYKRELYNICLDDLKGEEDETHIYVQK KVKDSWITLNDLFKETDLTGRPHIFAYVDVEEIIILLCEDEEFSNRKKDMTCHRFYSNDGKEY NNAEITISDYILKDKLLSSYVSLPLKIENREYFLICGVSPYKFKDDNKKDDILCMASHDKGETW GTKIVIKYDNYKLGVQYFFLRPYISKNDLSFHFYVGDNINNVKKNVFIECTHEKDLEFVCSNR DFLKDKNVLQDVSTLNDEYIVSYGNDNNFAECYIFFNENENSILIKPEKYGNTAAGCYGGTFVK IDENRALFIYSSSQGIYNIHTIYYANYEGGGGS EPEA
R58C	<u>MGWSCIIIFLVATATGVHSPDNKCDLSCPSNKCVCVIENGKQTCCKSERFVLENGVCICANDY</u> KMEDGINCIAKNKCKRKEYENICTNPNEMCAYNEETDIVKCECKEHHYRSSRGECILNDYCK DINCKENEECSIVNFKPECVCKENLKKNNKGECIYENSCLINEGNCPKDSKCIYREYKPHECV CNKQGHVAVNGKCVLEDGGGGSGGGGSAHIVMVDAYKPTKGGGGSGGGGSDSRHVFIRT ELSFINKNNVPCIRDMFFIYKRELYNICLDDLKGEEDETHIYVQKVKDSWITLNDLFKETDLTG RPHIFAYVDVEEIIILLCEDEEFSNRKKDMTCHRFYSNDGKEYNNAEITISDYILKDKLLSSYV LPLKIENREYFLICGVSPYKFKDDNKKDDILCMASHDKGETWGTKIVIKYDNYKLGVQYFFLR PYISKNDLSFHFYVGDNINNVKKNVFIECTHEKDLEFVCSNRDFLKDKNVLQDVSTLNDEYIV SYGNDNNFAECYIFFNENENSILIKPEKYGNTAAGCYGGTFVKIDENRALFIYSSSQGIYNIHTIY YANYEGGGGSEPEA

## Supplementary Information References

1. Alanine, D. G. W. *et al.* Human Antibodies that Slow Erythrocyte Invasion Potentiate Malaria-Neutralizing Antibodies. *Cell* **178**, 216–228 (2019).
2. Ragotte, R. J. *et al.* Heterotypic interactions drive antibody synergy against a malaria vaccine candidate. *Nat Commun* **13**, 1–12 (2022).
3. Chen, L. *et al.* An egf-like protein forms a complex with pfrh5 and is required for invasion of human erythrocytes by plasmodium falciparum. *PLoS Pathog* **7**, (2011).
4. Chen, L. *et al.* Structural basis for inhibition of erythrocyte invasion by antibodies to Plasmodium falciparum protein CyRPA. *Elife* **6**, (2017).
5. Jumper, J. *et al.* Highly accurate protein structure prediction with AlphaFold. *Nature* **2021 596:7873 596**, 583–589 (2021).
6. Douglas, A. D. *et al.* Neutralization of Plasmodium falciparum merozoites by antibodies against PfrH5. *Journal of immunology* **192**, 245–58 (2014).
7. Dreyer, A. M., Beauchamp, J., Matile, H. & Pluschke, G. An efficient system to generate monoclonal antibodies against membrane-associated proteins by immunisation with antigen-expressing mammalian cells. *BMC Biotechnol* **10**, 1–14 (2010).
8. Dreyer, A. M. *et al.* Passive Immunoprotection of Plasmodium falciparum -Infected Mice Designates the CyRPA as Candidate Malaria Vaccine Antigen . *The Journal of Immunology* **188**, 6225–6237 (2012).